Xin Tan, Zhi Sun, and Ian F. Akyildiz

Wireless Underground Sensor Networks

MI-based communication systems for underground applications.

Wireless underground sensor networks (WUSNs) can enable many important applications such as intelligent agriculture, pipeline fault diagnosis, mine disaster rescue, concealed border patrol, and crude oil exploration. The key challenge to realize WUSNs is the wireless communication in underground environments. Most existing wireless communication systems utilize a dipole antenna to transmit and receive propagating electromagnetic (EM) waves, a method that does not work well in underground environments due to the high material absorption loss. The magnetic induction (MI) technique provides a promising alternative solution that could address the current problem in underground environments. Although MI-based underground communication has been intensively investigated theoretically, little effort has been made so far to develop a testbed for MI-based underground communication that can validate the theoretical results. In this article, a testbed of several MI-based communication systems is designed and implemented in an in-lab underground environment. The testbed realizes and tests not only the original MI mechanism utilizing a single coil but also recently developed techniques that use the MI waveguide and three-directional (3D) MI coils. The experiments are conducted in an in-lab underground environment with reconfigurable environmental parameters, such as soil composition and water content. This article provides the principles and guidelines for developing the MI underground communication testbed, which is very complicated and time consuming due to the new communication mechanism and the new wireless transmission medium.

Digital Object Identifier 10.1109/MAP.2015.2453917
Date of publication: 24 August 2015

A WUSN is implemented to monitor underground tunnels to ensure safe working conditions in coal mines.

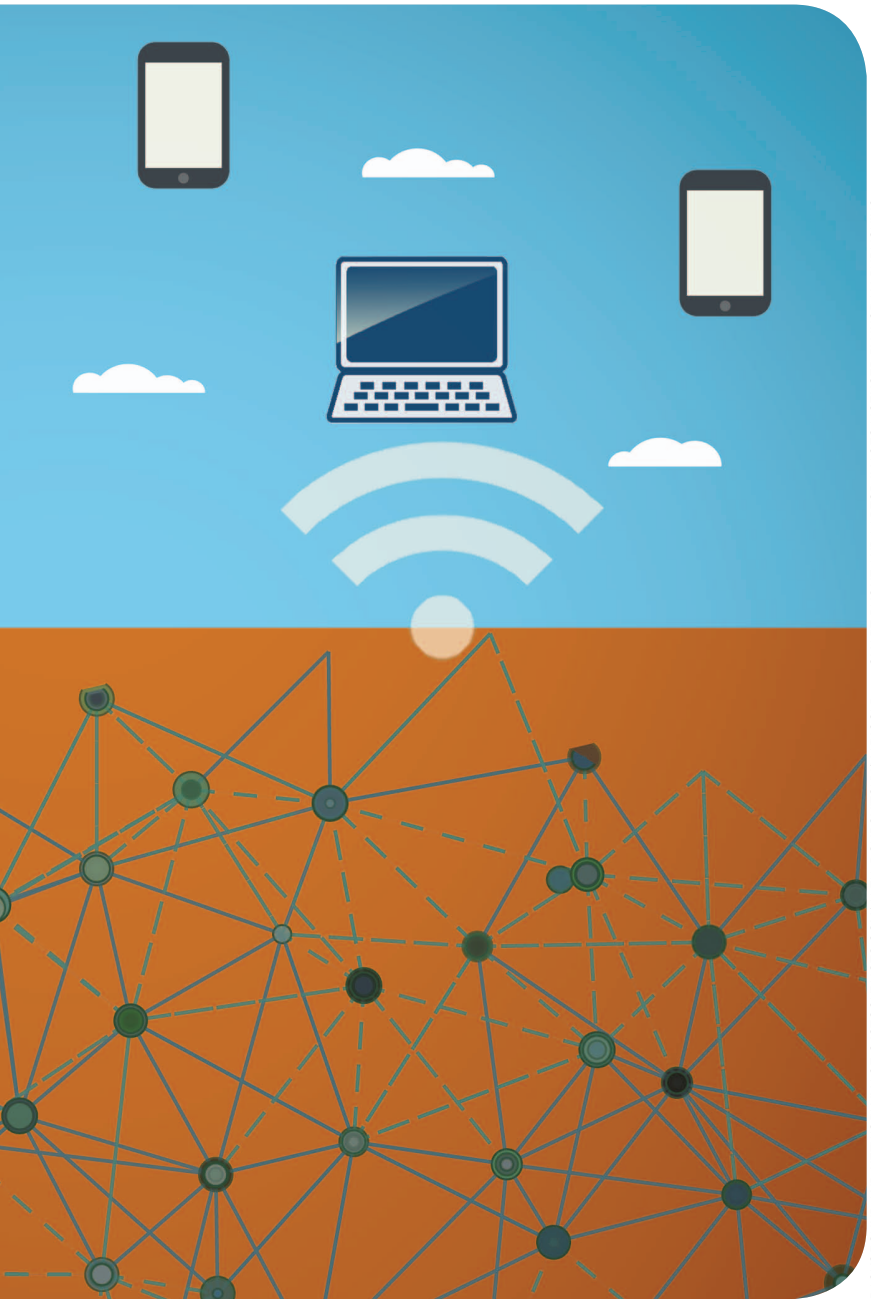

BACKGROUND AND NETWORK IMAGE © ISTOCKPHOTO.COM/ ALEX_DOUBOVITSKY/MARIGOLD_88 SMART PHONE AND LAPTOP IMAGES LICENSED BY INGRAM PUBLISHING

Underground wireless communication is the enabling technology to realize WUSNs, which can be used in a wide variety of novel applications, including intelligent agriculture, pipeline fault diagnosis, mine disaster rescue, concealed border patrol, and crude oil exploration [1]–[7].

Underground environments are more complicated than aboveground environments as they contain air, sand, rocks, and water with electrolytes. It is challenging to realize wireless communication in such complex environments. Classic techniques based on EM waves are widely used in terrestrial environments. However, those techniques do not work well in underground scenarios. First, EM waves experience high levels of attenuation due to absorption by soil, rocks, and water underground [8]. Second, the electrolytes in the underground medium become the dominating factor that influences the path loss of EM waves. As a result, soil water content, density, and makeup can affect the performance of communication unpredictably since these factors change with location and vary dramatically over time. Third, operating frequencies in megahertz or lower ranges are necessary to achieve a practical transmission range [8], [9]. Thus, compared with the communication range, the antenna size will become too large to be deployed underground.

Alternative communication techniques using MI provide promising properties that can solve the problems mentioned above. Instead of using propagating EM waves, MI techniques utilize the near field of the low-frequency EM field to realize wireless communication. Since any such technique is based on the MI between two coupled coils, it is not influenced by the complicated underground medium because the magnetic permeability of soil is almost the same as that in air. Moreover, MI communication can effectively transmit and receive wireless signals using a small coil of wire. Hence, the problem of antenna size can be solved.

Theoretical research on MI underground communication has developed quickly in recent years, but the implementations and validations are seldom developed. Although significant improvements can be achieved using MI techniques in theory, the theoretical prediction may be biased due to

ideal assumptions that are difficult to realize in practical deployment. To this end, a testbed should be designed and implemented to evaluate MI-based wireless communications in real underground environments. An integrated system, including the signal generator, transceivers, reconfigurable underground environment, and observation strategies, needs to be realized.

In this article, we present the development of an MI-based underground communication testbed as well as the experiments and measurements derived by the developed testbed. In particular, the testbed implements not only the original MI communication mechanism, where only a single coil is used for each transceiver, but also a more advanced MI system where the MI waveguide [8], [10], [11] is used to extend the communication range and 3D MI coils [3] are used for omnidirectional coverage. The modules in the testbed design include the MI coil, signal generation and observation, and underground environment construction. In the MI coil design module, we first use two coupled coils as the original form of MI communication. Then, the MI waveguide and 3D MI coils are tested. In the signal generation and observation module, we use universal software radio peripherals (USRPs) [12] to build an integrated communication system. To construct a reconfigurable underground environment in the laboratory, 980,000 cm^3 of sand was poured in a 255-cm long tank to form the base material of the underground medium. A water cycle is built to keep the dynamic balance of water in the tank. Measurements such as path loss, bandwidth, and packet error rate (PER) are then taken in the testbed for variance system and environmental configurations. Based on the experiments, we evaluate the accuracy of previous theoretical models and compare our results with the EM wave-based system.

RELATED WORK

The concept of WUSNs is first introduced in [4], after which many novel applications are presented based on WUSNs. In [5], a WUSN is implemented to monitor underground tunnels to ensure safe working conditions in coal mines. In [3], the WUSNs are deployed during the hydraulic fracturing process in crude oil extraction, which can provide real-time physical and chemical measurements deep inside oil reservoirs. In [6] and [7], the WUSNs are utilized for pipeline leakage detection where MI communications are used to connect the sensors along pipelines.

To set up the theoretical fundamentals of the wireless underground communication, the channel models for the propagation of EM waves in underground environments are discussed in [9], [13], and [14]. An EM wave-based underground communication testbed is developed in [15]. The results from the testbed show that if there is no above ground device, the EM wave-based communication in pure underground channel encounters prohibitively high path loss.

MI techniques are introduced to wireless underground communication in [8], [10], and [16]. The MI techniques are shown to provide a more reliable underground communication channel. However, MI communication has a limited communication range due to the high attenuation rate in the near region. The MI waveguide concept is originally developed in [17]–[22], in which it is used for artificial delay lines and filters, dielectric mirrors, distributed Bragg reflectors, and slow-wave structures in microwave tubes. The channel model for both original MI communication and MI waveguide are maturely developed in recent years [8], [10], [11], [16]. A model of 3D MI communication, is also introduced in [3].

Despite the active theoretical research, the implementations and experimental results on MI underground communications are seldom developed. However, implementations of MI techniques have been done in areas other than communications. In [23], MI techniques are used to create a charger along the railway that charges trains. In [17] and [24]–[28], two coupled MI coils are used to transfer the electric power between portable wireless devices. In [17] and [26], the MI waveguide with strong coupled neighbor coils is tested. Out of these applications, however, none has been used to evaluate MI-based communications.

Moreover, those experiments on MI techniques are conducted in the air medium. No experiments have been done on MI communication performance in the more complicated underground medium.

To this end, in this article, we develop a testbed for MI underground communication to evaluate the previous theoretical results and provide the experimental platform for future MI communication research.

SYSTEM DESIGN

Implicit in the concept of an underground communication system is that the communication occurs entirely using underground propagation media. To implement and test such underground-to-underground communication, a testbed should contain three modules: an underground antenna, signal generation and observation, and the in-lab underground environment. Based on these three modules, the architecture of underground communication testbed can be developed, as shown in Figure 1. Two new designed devices, performing as the antennas, are buried in the in-lab underground environment. The signal generation and observation modules, used for signal generation and taking measurements, are connected to the antennas. The

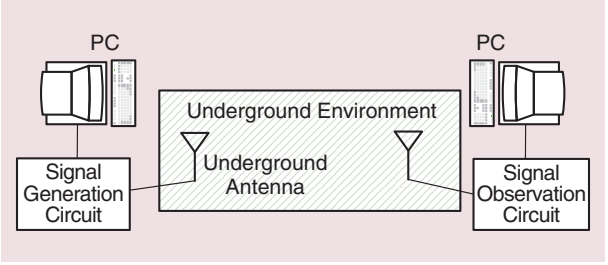

FIGURE 1. The architecture of the underground communication testbed. PC: personal computer.

initial objective of this testbed is to establish MI underground communication and to evaluate the performance by measuring important characteristics such as path loss, bandwidth, and PER.

WUSNs can enable many important applications such as intelligent agriculture, pipeline fault diagnosis, mine disaster rescue, concealed border patrol, and crude oil exploration.

UNDERGROUND MI COIL DESIGN

ORIGINAL MI COMMUNICATION

The MI coil plays the most important role in the underground communication system since traditional antennas like electrical dipoles cannot provide reliable communication in such a complicated propagation medium. As shown in Figure 2(a), the transmission and reception are accomplished with the use of a coil of wire. A photo of MI transceivers used for this testbed is shown in Figure 2(b). In this testbed, the MI coils are fabricated with eight-turn coils wound on square frames with an edge length of 10 cm. A 26-American wire gauge (AWG) wire that provides a unit length resistance of 0.1339 Ω/m is used. A variable series capacitor, from 10 to 230 pF, is welded in the circuit for resonance.

The ratio of the received power to the transmitted power based on the channel model is developed in [8]. Based on this channel model, to increase the channel gain, we can either enlarge the size of the coils or increase the number of turns; however, this enlarges the transceiver. Other than the coil size and number of turns, the unit length resistance of the loop also has a significant influence on the channel gain. Thus, we can use the low resistance wires and circuit to reduce the path loss without increasing the size. To reduce the wire and circuit resistance, we can select high conductivity wires, better connecters, better capacitors, and a customized printed circuit board (PCB).

Although the MI system in its original form has constant channel condition and a relatively longer transmission range than the EM wave-based system, its transmission range is still too short for practical applications [7], [16]. Moreover, the communication performance of an ordinary MI coil is influenced by the intersection angle of two coils so that transceivers can only be deployed face-to-face in a straight line to get the maximum signal strength at the receiver side. To enlarge the communication range and increase the degree of freedom of transceiver deployment, the MI waveguide and 3D MI coils can be used.

MI WAVEGUIDE

The MI waveguide consists of a series of relay coils between two underground transceivers [16]. Different from the relays using EM wave techniques, an MI relay is just a simple coil without any power sources or processing devices. The MI waveguide and the regular waveguide are based on different principles and are suitable for different applications. The MI waveguide is based on the induction coupling between a series or array of independent coils. The communication technique using the MI waveguide belongs to wireless communication although some relay coils are deployed between the transceivers. Because of this physical structure, the MI waveguide has a high degree of freedom of deployment and utilization in many harsh environments, such as underground environments. Figure 3(a) gives a view of MI waveguide

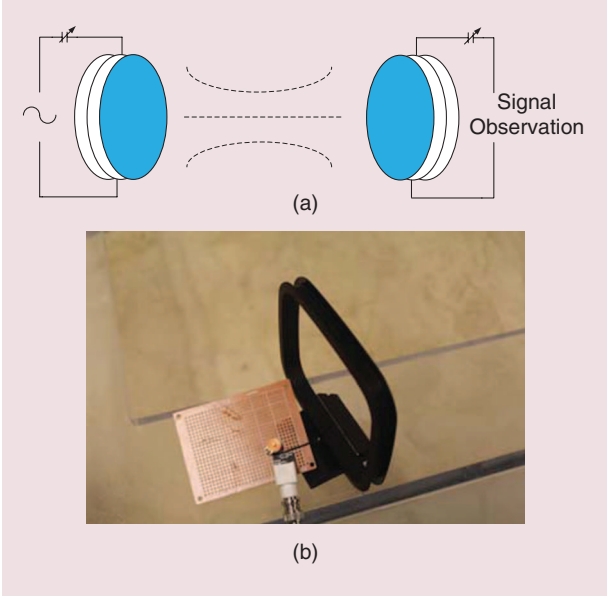

FIGURE 2. Wireless communication based on MI: (a) MI-based wireless communications and (b) an MI coil.

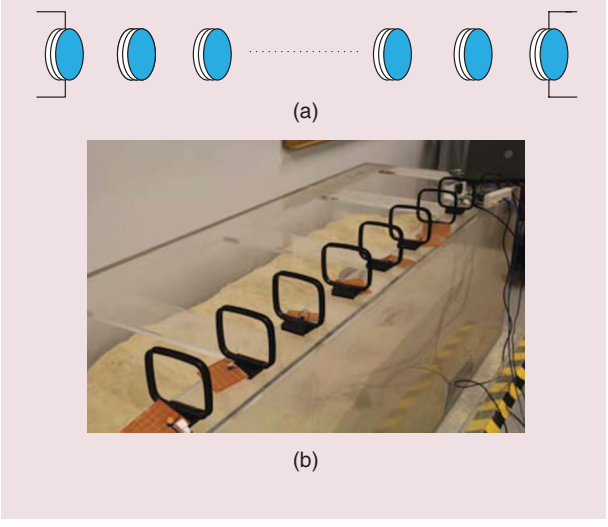

FIGURE 3. An MI waveguide based on relays: (a) a diagram of the MI waveguide and (b) a photo of the MI waveguide.

formed by relays. Since the MI transceivers and relays are coupled by deploying in a straight line, the relays will get the induced currents one by one until each reaches the receiver. The signal strength at the receiver side gets larger during this process. Figure 3(b) shows the MI waveguide used in this testbed.

In this testbed, six coils are deployed between the MI transceivers to serve as the MI relays. Each relay is fabricated using 26-AWG wire and a series capacitor, which are the same as the transceivers. The only difference is that relays are closed-loop circuits without any power input. According to the channel gain of the MI waveguide developed in [8], to get a significant increase in signal strength with a communication distance of 2 m, six or more relays are necessary. The density of relays can be reduced if we reduce the unit length resistance for each coil using high-conductivity wires and PCBs.

Underground environments are more complicated than aboveground environments as they contain air, sand, rocks, and water with electrolytes.

3D MI COIL

For the MI transceivers, the received signal strength is influenced by the angle between the axes of two coupled coils. However, usually underground MI coils need to be deployed in a complicated situation, such as when multiple coils are not kept in a straight line. To maintain high-quality communication in such a complicated situation, an improvement using multidimensional MI coils is developed in [3]. To achieve omnidirectional coverage with a minimum number of coils to reduce the system complexity and cost, 3D MI coils designed in [3] are used in this testbed. An example of a 3D coil is shown in Figure 4, where three independent coils are fabricated and installed vertically on a cube with an edge length of 10 cm. Each of the three coils can form a strong beam along each of the three axes in the Cartesian coordinate. Due to the field distribution pattern of the coil, the orthogonal coils on the same wireless device do not interfere with each other since the magnetic flux generated by one coil becomes zero at the other two orthogonal coils. Just as with the original MI coils, 26-AWG wire is used for the 3D coil fabrication, and each coil is equipped with a series capacitor for finding resonance. At the receiver side, three signals from three independent coils are added together. Based on the developed channel model, once the parameters of MI coils and communication distance are fixed, how much signal strength we can get depends on the intersection angle between the transmitter and receiver. Using three orthogonal coils, at least one coil can get enough signal strength no matter how we change the intersection angle. The system is supposed to keep a high degree of communication when rotating the MI coils and changing the intersection angle between them.

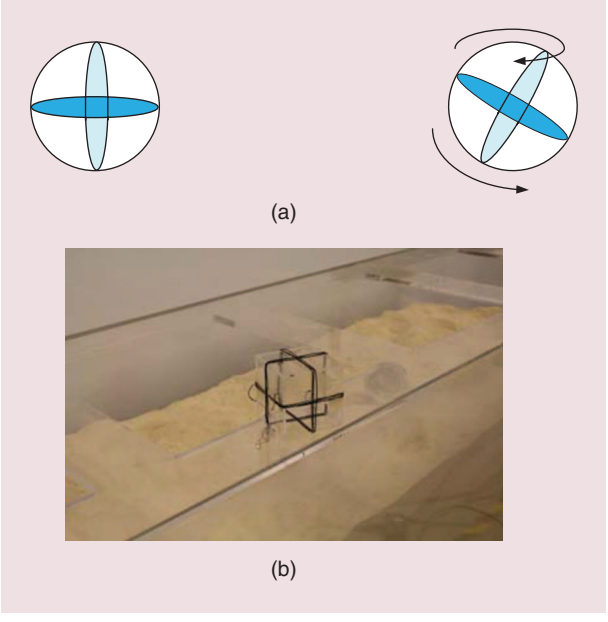

FIGURE 4. 3D MI communication: (a) a diagram of 3D MI communication and (b) a photo of the 3D MI coil.

SIGNAL GENERATION AND OBSERVATION

To implement the designed MI coils in underground environments, a signal generator and a method to observe the received signal are needed. A signal generator and an observer can be formed by modules, as shown in Figure 5.

The first module in Figure 5 is the interface to the PC, which is connected to a laptop with a non-Unix (GNU) radio installed. The laptop with GNU radio is used to generate data sources and provide the coded information to the signal generation circuit though the interface. At the receiver side, the GNU radio is also used for signal monitoring. The GNU radio is an open-source software that achieves the entire signal-processing procedure before the transmission. In GNU radio, basic blocks are provided by the built-in library. These blocks are written in C++ and are connected using Python with the help of open-source SWIG tools. Blocks can also be created using C++ and added to the library if needed. The GNU radio also has a graphical user interface and a GNU radio companion (GRC). The GRC is a graphical user interface via which different blocks can be connected and then the codes generated in Python according to the connected blocks. These GRC blocks are used in our experiment to send digital signals and read the data at the receiver side.

Figure 6(a) shows a flowgraph of signal generation. In this flowgraph, the generated signal is defined by the signal

source block. Here, we simply use a sinusoidal waveform. The channel gain is defined in a USRP sink block connected to the signal source. The operating frequency, as well as the sampling rate, can be defined in these GRC blocks. However, this signal generation flowgraph is only used for system correction such as finding the resonance. For further measurements, especially the PER, more complicated signal packets should be sent.

Figure 6(b) and (c) show, respectively, the signal observation in the time and the frequency domains at the receiver side. In Figure 6(b), a USRP source block is used to get the information from the receiver USRP. A scope sink block is connected directly to show the received signal in the time domain. Two independent streams can be read on this scope so that it is convenient for testing multiple MI coils at the same time. In Figure 6(c), a fast Fourier transformation (FFT) block is added between the USRP source and the scope sink since we need to transform the received signal from the time domain to the frequency domain and display it in decibel-milliwatt by taking the logarithm. In this flowgraph, we also define two independent channels for signal observation.

The field-programmable gate array (FPGA) module in Figure 5 provides the signal processing and digital up-conversion and interpolation capabilities. After the FPGA, the digital-to-analog converter (DAC) module is used to convert the processed digital information to an analog signal that will be input to the transmitting RF front end. At the receiver side, the received signal samples are sent to the analog-to-digital converter (ADC) module that decimates and downconverts the received signals from the receiving RF front end. Further downconversion is done by the FPGA, and the samples are sent through the gigabit Ethernet. The FPGA and DAC/ADC blocks can be realized by USRP motherboards [12]. In this testbed, the USRP N210 used is equipped with a Xilinx Spartan-3A DSP 3400 FPGA, a 100-MS/s dual ADC, a 400-MS/s dual DAC, and gigabit Ethernet connectivity to stream data to and from host PCs.

The RF front-end module in Figure 5 is used to prepare the signal for wireless transmission and input the signal to the MI coil. In the testbed, the daughterboard of USRP is used as the RF front end, which can modulate the output baseband signal to the transmission frequency or convert the received signal back to the baseband. The LFTX/LFRX daughterboards used in this testbed support transmitting and receiving signals from 0 to 30 MHz. Each LFTX/LFRX daughterboard can support two independent antennas by two antenna connectors, transmitter A/receiver A and transmitter B/receiver B. A photo of the USRP motherboard equipped with a daughterboard is shown in Figure 7.

UNDERGROUND ENVIRONMENT CONSTRUCTION

Since the testbed aims to evaluate underground MI communications, an underground environment in the laboratory is needed. In our implementation, an acrylic tank 255 cm × 76 cm × 76 cm (length × width × height) was assembled on a pedestal. About 980,000 cm^3 of sand was poured into the tank, serving as the base material for the underground environment. The underground soil medium contains a certain concentration of water with electrolytes, which is the dominant factor that can influence the performance of underground communication systems. Hence, in the underground environment of the testbed, water should be poured and mixed with the sand. As shown in Figure 8, due to the weight and percolation, the water sinks to the bottom of the tank and cannot be automatically and uniformly distributed. To address this problem, small holes are opened on the bottom of the tank so that the water can leak out of the pedestal. A dirty-water pump is used to pump the water back into the tank from the top. Thus, the water can be circulated inside the tank so that the soil–water content is dynamically balanced. In this testbed, water is measured by a measuring cylinder and uniformly mixed with the sand to get a certain water content.

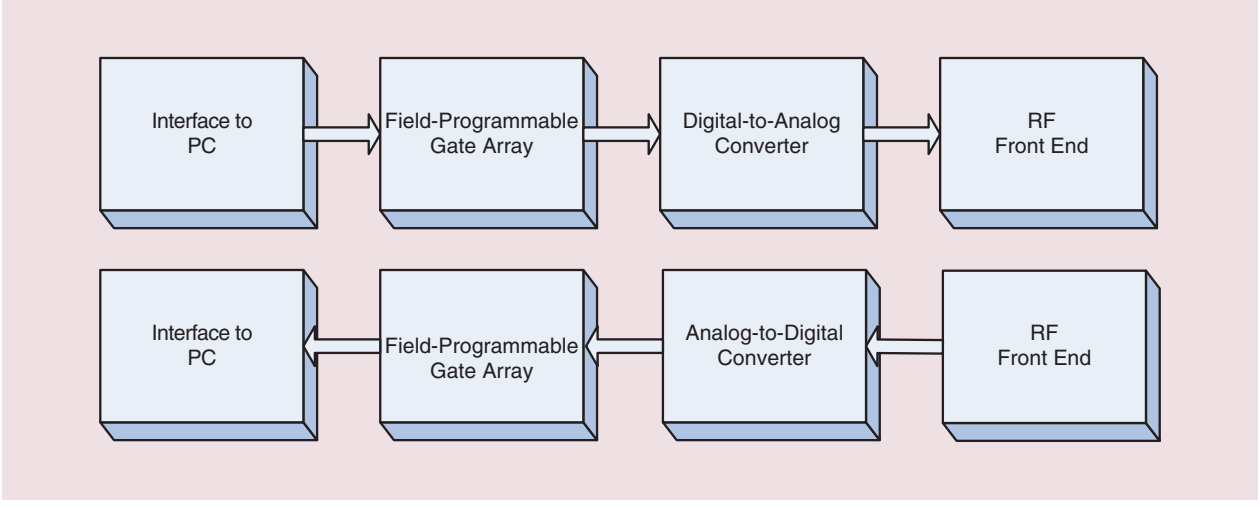

FIGURE 5. The signal generation and observation design.

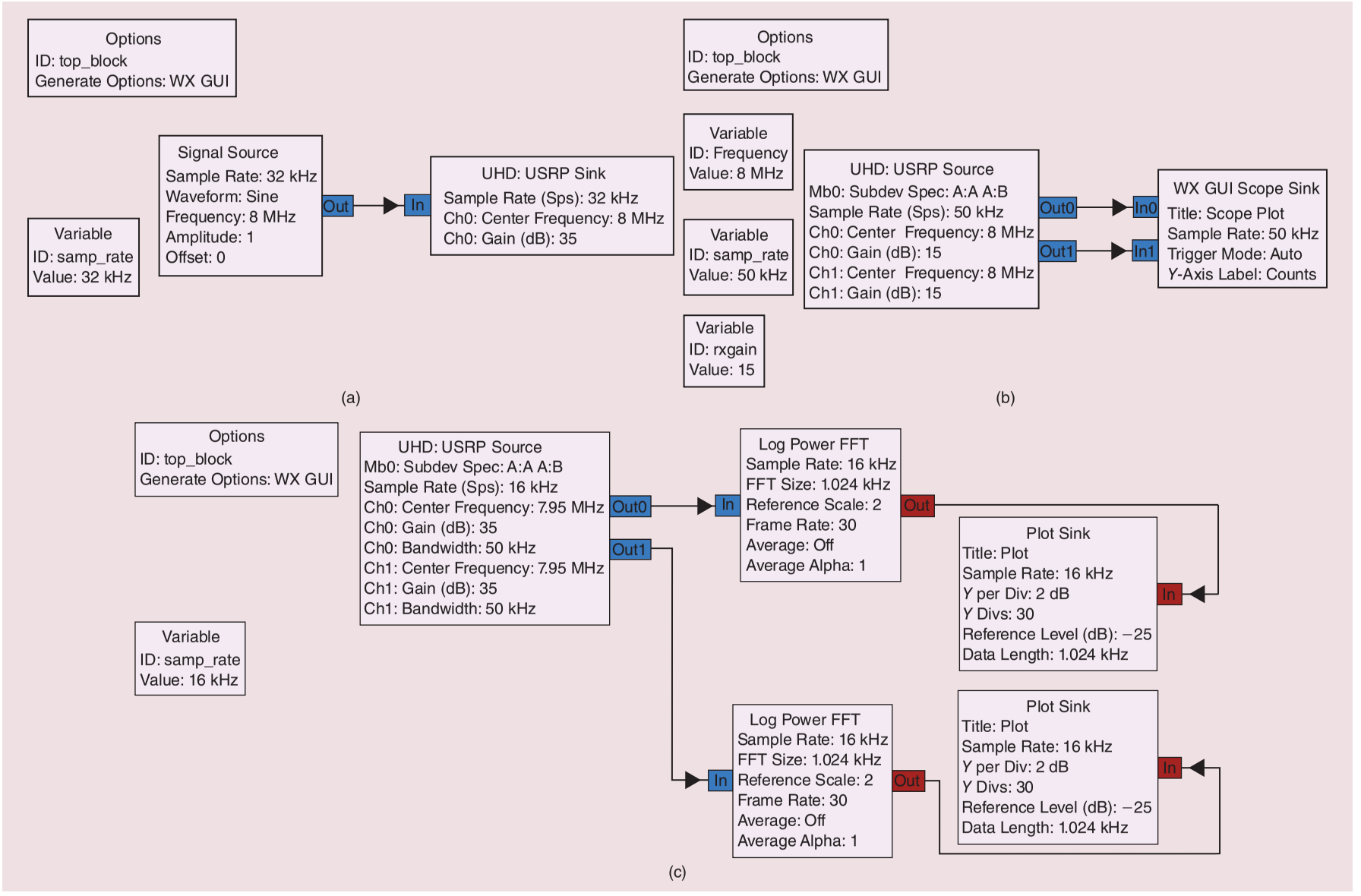

FIGURE 6. The signal generation and observation illustrated by GRC flowgraphs. (a) A flowgraph of signal generation, (b) a flowgraph of signal observation in the time domain, and (c) a flowgraph of signal observation in the frequency domain. FFT: fast Fourier transformation; ID: identification; GUI: graphical user interface; UHD: universal hardware driver.

Figure 9(a) shows the method used to deploy the MI coils in the underground environment. MI coils are deployed and buried inside tank. Each coil is covered with water-resistant bags to prevent the devices from being damaged by the water and sand. The MI coil is connected to the USRP daughterboard by a shielded coaxial cable to guarantee that there is no wireless signal radiation from any components other than the coil. A photo of the in-lab underground environment is shown in Figure 9(b).

EXPERIMENTS AND DISCUSSION

To test the performance of MI underground communication in the soil medium with different concentrations of water, we test the volume water content (VWC) at 0, 5, 10, and 20%. Because of the slow evaporation of water, usually the variation of VWC from 0 to 20% is irreversible in a short time. For each VWC, we take measurements including path loss, bandwidth, and PER with various communication distances. Each set of data is independently measured ten times.

A flowchart of operating steps is shown in Figure 10. First, all the measurements are taken in dry sand. To evaluate the communication performance against the communication range, we vary the distance between transceivers from 20 to 220 cm, and measurements are taken ten times for each communication distance. After finishing all the measurements in dry sand, we increase the VWC to 5, 10, and 20%, successively, and redo the steps. During the experiment with water inside the tank, a water pump, as mentioned in the "System Design" section, keeps working to maintain a constant VWC. Here, the default system configuration includes 8-MHz operating frequency, eight-turn MI coils, and 0% VWC, if not otherwise specified.

Figure 11 shows the experimental results derived from the testbed where the MI communication in the original form (a single MI coil) is tested in 0% VWC. The x- and y-axis, respectively, show the distance between the transmitter and receiver, and the signal strength received at the receiver side. The operating frequency is 8 MHz in this experiment. As shown in Figure 11, the curve with crosses represents the average received power taken at the receiver side, and the smooth curve is the calculated result based on the theoretical model. Since the measurements are taken ten times at each communication distance, bars on the curve show the maximum and minimum values in each group of data. The experimental result shows a good match with the theoretical calculation. It should be noted that the path loss can be further reduced using low resistance coils and circuits, which can move the curves in Figure 11 upward; however, the attenuation speed of the curve will not change.

Figure 12 shows the received power with operating frequency variation. Compared to 8 MHz, the signal strength is a little lower using 6 or 4 MHz. As mentioned previously, to maximize the signal strength in both the transmitter and receiver, a series variable capacitor is welded in each circuit so that the circuit impedance can be minimized by finding the resonance. According to the equivalent resistance-inductance-capacitance circuit developed in [8], since the inductance of the circuit is already determined by the coil fabrication, to cancel the effect of inductance and get

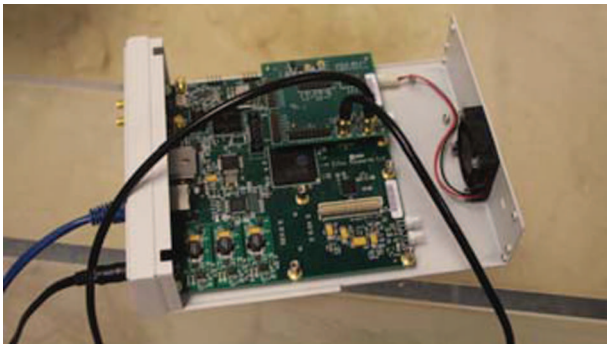

FIGURE 7. A photo of the USRP equipped with a daughterboard.

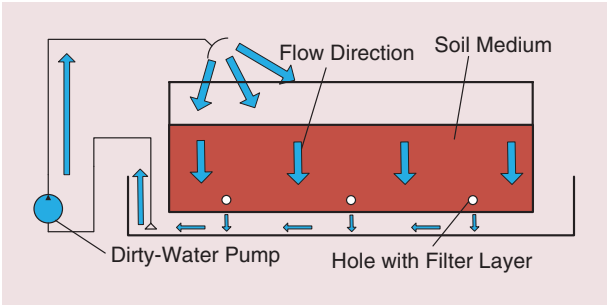

FIGURE 8. A water cycle for the in-lab underground environment.

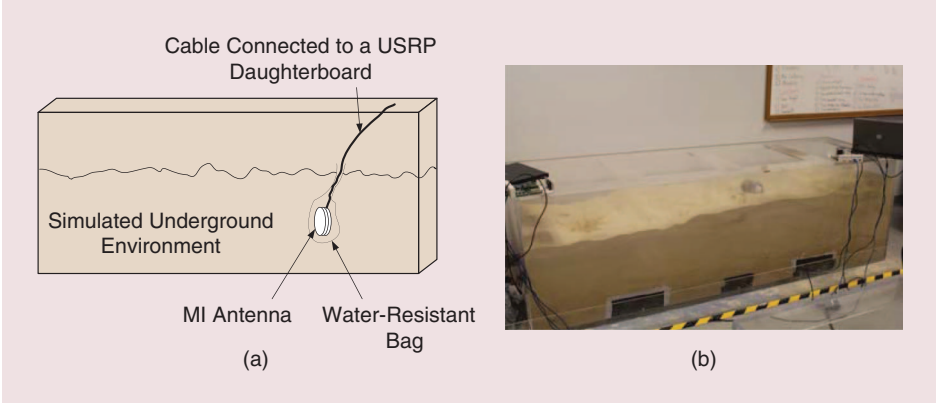

FIGURE 9. The MI coil in the underground environment: (a) MI coil deployment and (b) the in-lab underground environment.

the resonance, the value of the capacitor should be changed with frequency variation. However, restricted by the range of series capacitance, the operating frequency can only be taken from 4 to 9 MHz.

The bandwidth of the MI communication with the MI coil is shown in Figure 13. We find that the bandwidth of the MI system does not obviously change in the distance range that the in-lab underground environment provides. The measurements in Figure 13 are taken by using a communication distance of 2 m. To find the bandwidth, series capacitors on the MI coil circuits are adjusted for a certain operating frequency (8 MHz) at the beginning. Then the operating frequency is changed to get the decreased signal strength. During the frequency changing, the capacitors are fixed. The bandwidth is then derived by measuring the width of the frequency band where the received signal strength is within a 3-dB range from the peak. From Figure 13, we find that the bandwidth is about 0.02 MHz, which is very close to the calculated result.

The MI technique provides a promising alternative solution that could address the current problem in underground environments.

The experimental results of MI communication in underground environments with different water contents are shown in Figures 14 and 15. Figure 14 shows the comparison between the experimental result and calculated result in different VWC underground environments. The communication based on EM waves is also measured to make a comparison in Figure 15. For the EM power measurements, VERT2450 antennas are used at 2.45-GHz operating frequency. The VERT2450 antennas are dual-band omnidirectional antennas at 3-dBi gain. The other signal generation and observation modules are the same as those used for MI communication. Compared with the communication based on EM waves, even without antenna gain, MI communication shows significant benefits in underground environments. For 5% VWC, the received signal strength using MI communication is about 10 dB higher than it is using EM waves with a communication of 0.2 m. The difference increases over 20 dB if the communication distance is 1.8 m. More benefits can be derived if we increase the VWC to 10 and 20%. For 20% VWC, the EM-based communication suffers a high attenuation ratio; the received signal strength is close to –90 dBm with a distance of 1 m. However, by using MI communication, the signal strength is 30-dB higher in this case.

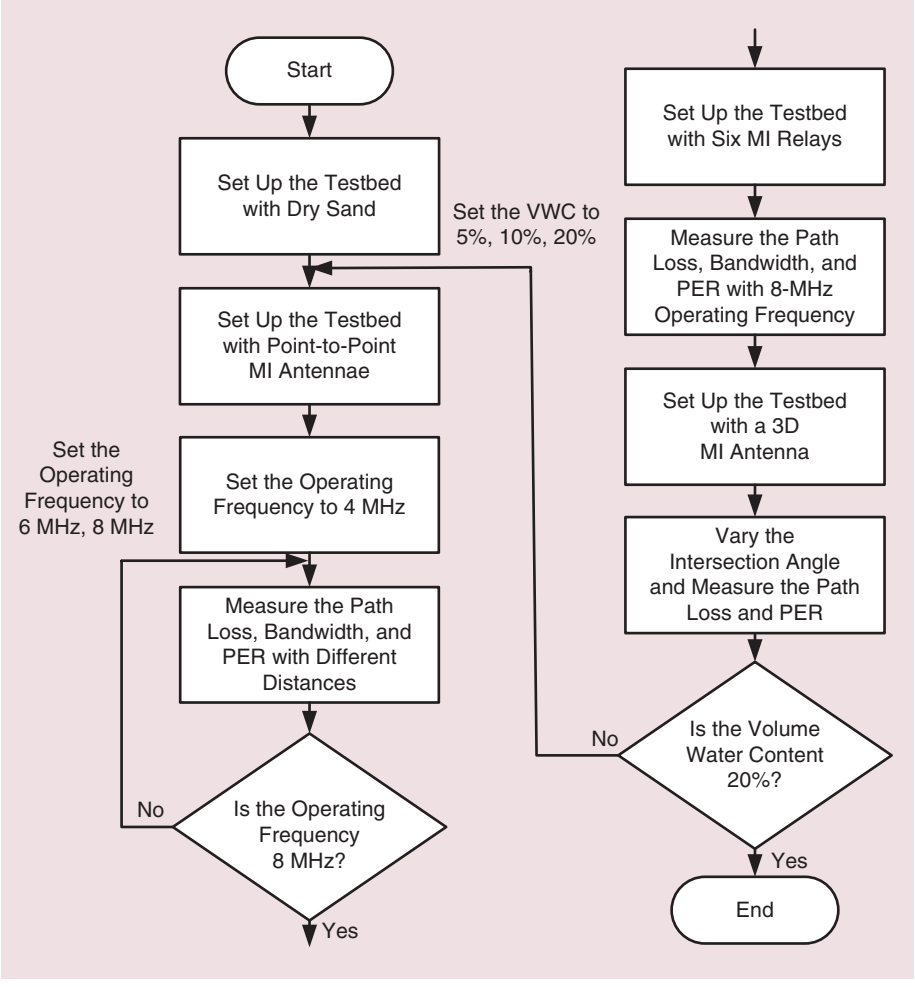

FIGURE 10. A flowchart of operating steps.

Figure 16 shows the comparison of PER in logarithmic scale between MI communication and EM wave communication in different underground environments. For the MI communication, PER increases as VWC increases, and it becomes obvious after a distance of 2 m. Thus, the communication range using this pair of MI coils is around 2 m. For the

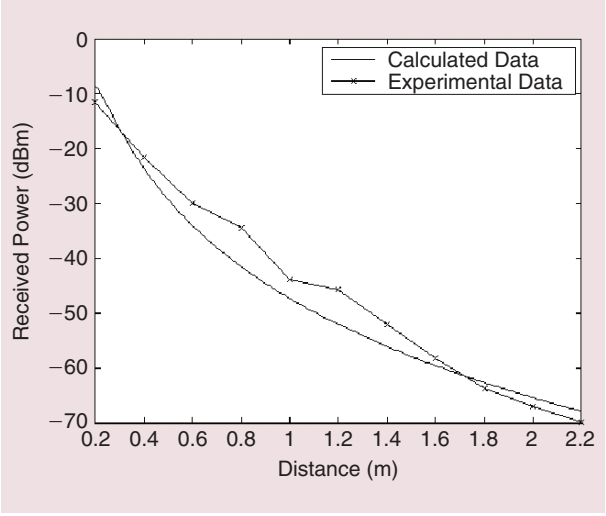

FIGURE 11. The received signal strength of the original MI communication.

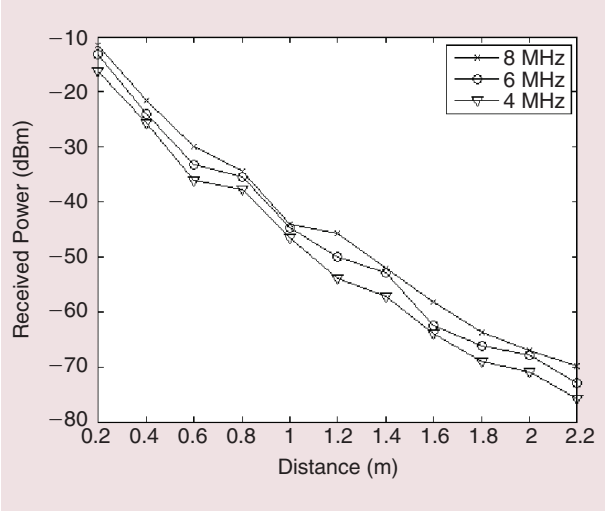

FIGURE 12. The received signal strength for different operating frequencies.

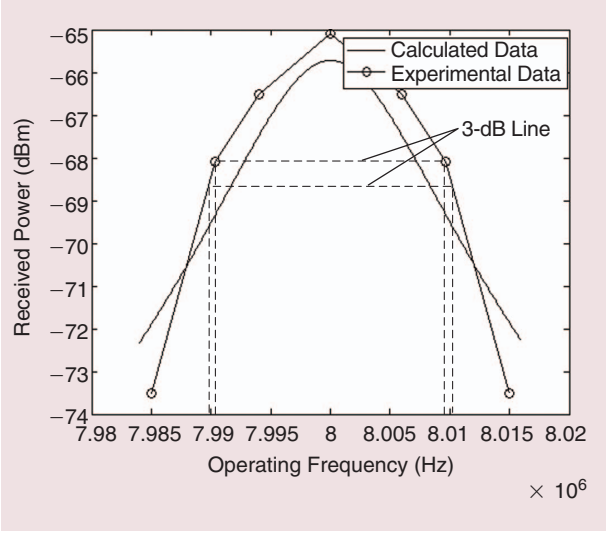

FIGURE 13. The bandwidth of the original MI communication.

communication using EM waves, the PER is much higher than it is when using MI communication, and it is dramatically influenced by the VWC change. In a 20% VWC environment, even within a short distance of 1 m, the PER is over 10%, and a satisfying level of communication can hardly be established in this case.

A comparison between the original MI communication and the MI waveguide is shown in Figure 17. By deploying six relays between the transmitter and receiver, the gap between the two curves obviously shows the benefits of using MI. Compared with the calculated result, the performance of MI waveguide in different underground environments is shown in Figure 18. Although the path loss increases as VWC increases, the MI waveguide has a good performance even in a high VWC of 20%. A comparison of bandwidth between original MI communication and the MI waveguide with six relays is shown in Figure 19. Experiments with 5, 10, and 20% VWC are successively used to

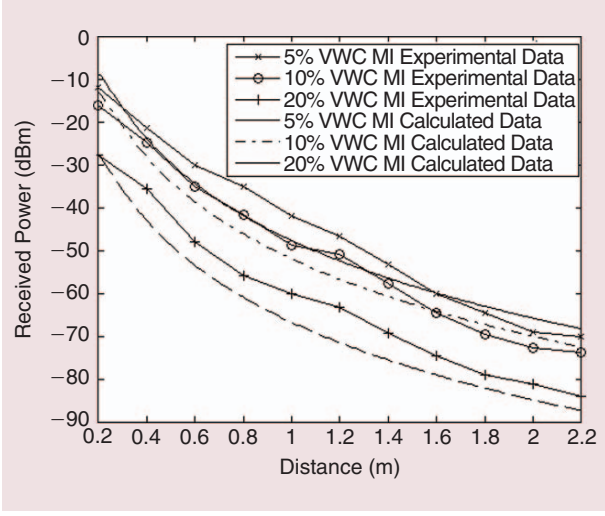

FIGURE 14. The received signal strength in underground environments with different VWCs.

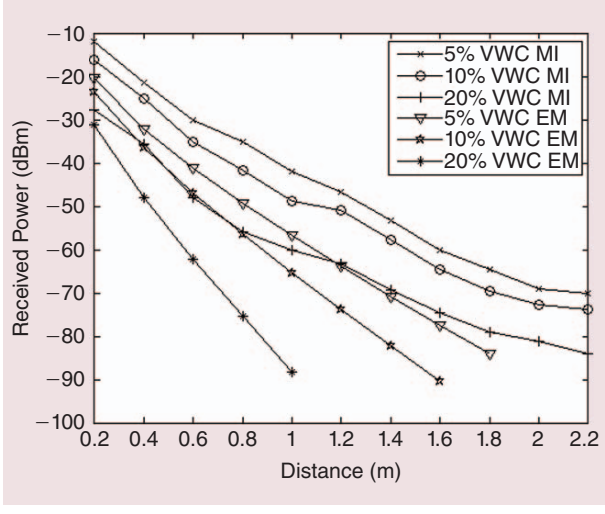

FIGURE 15. A comparison of received signal strength between MI and EM in underground environments.

get three comparisons. Compared with the bandwidth of original MI communication, the disadvantage of MI waveguide is not obvious if the MI relays are well fabricated with the same parameters and deployed with equivalent intervals.

Once the received signal strength and bandwidth are determined for both original MI and MI waveguide, the channel capacity of the underground MI communication can be derived. Based on the Shannon theorem, the channel capacity can be calculated by substituting the experimental results into the formula $C = W\log(1 + S/N)$, where C is the channel capacity, W is the bandwidth, and (S/N) is the signal-to-noise ratio. For example, since the measured background noise is around −90 dBm, by deploying the MI transceivers with a distance of 2 m in dry sand and using an operating frequency of 8 MHz, a channel capacity of 448,840 b/s can be derived. The channel capacity of the MI waveguide can be calculated the same way. By deploying the MI transceivers at a distance of 2 m with six relays between them in dry sand, a channel capacity of 608,000 b/s is derived.

The performance of the MI waveguide is significantly better than the original MI system since the MI waveguide dramatically increases the received power.

Figure 20 shows the channel capacities of MI communication in underground environments with different

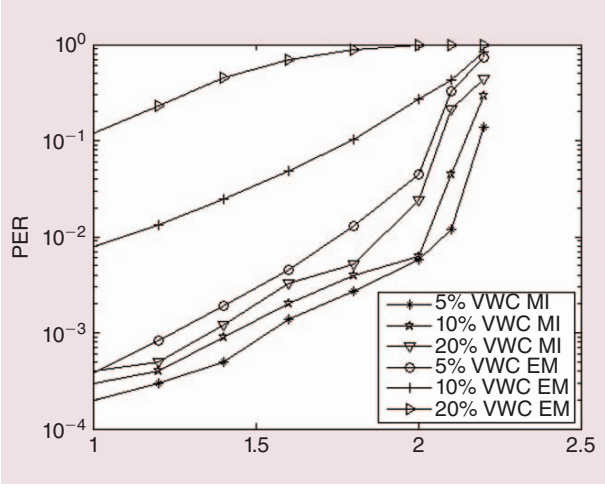

FIGURE 16. A comparison of PER between MI and EM in underground communication.

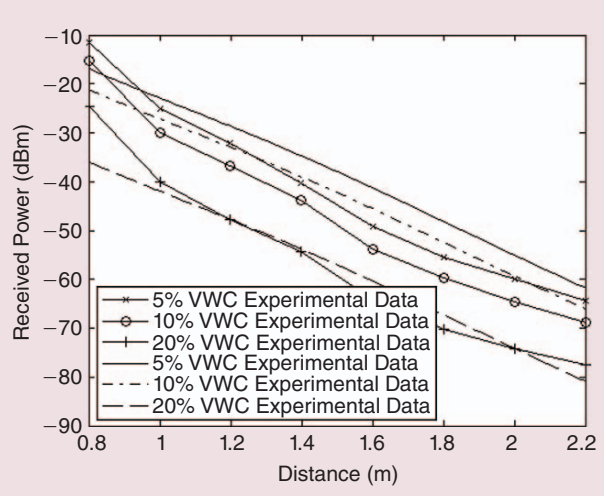

FIGURE 18. The MI waveguide in underground environment.

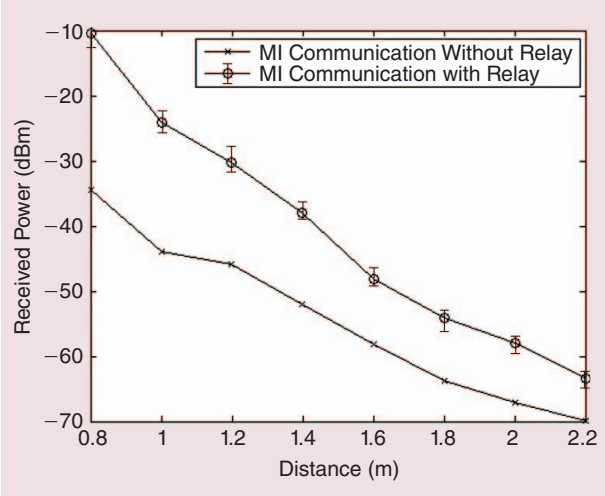

FIGURE 17. A comparison of received signal strength between original MI communication and the MI waveguide.

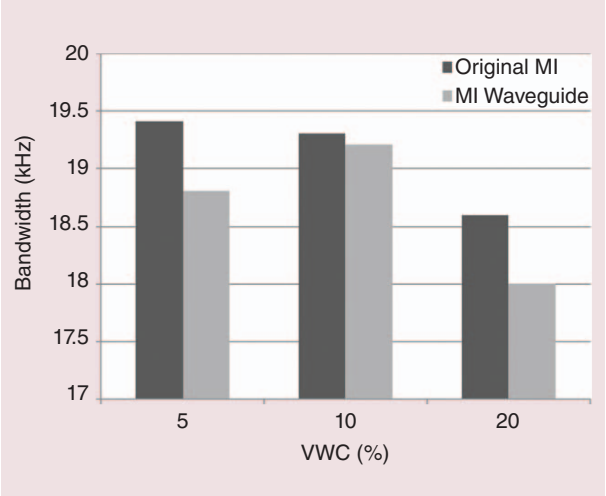

FIGURE 19. A comparison of bandwidth between original MI communication and the MI waveguide.

VWCs. For the MI waveguide, we take measurements with a starting distance of 0.8 m since six relays are deployed between transceivers and a necessary distance is kept for two adjacent coils. Since the noise level is a constant, the channel capacity only relies on the bandwidth and received signal strength. For the bandwidth, the difference between using original MI and the MI waveguide is not obvious. Moreover, according to the experimental results, the variation of bandwidth is not significant with the changes of VWC and communication distance inside the sand tank. Thus, the received signal strength becomes the dominating factor that influences the channel capacity. As shown in Figure 20, the performance of the MI waveguide is significantly better than the original MI system since the MI waveguide dramatically increases the received power. As expected, the channel capacities of both systems become smaller if we increase the VWC to 20%, due to the higher path loss in wet soil.

The advantages of the MI waveguide are also shown in terms of PER, as illustrated in Figure 21. The PER of the MI waveguide keeps a low level throughout all of the experiments. The communication range of the MI waveguide is larger than the length of this testbed, i.e., the length of the tank. Because of the relatively high resistance of wire we used to fabricate the MI coils, nontrivial energy is consumed in these relays. Hence, the experiment results are not the best performance we can have for the MI waveguide. Improvements can be achieved using a customized PCB circuit and more efficient experimental supplies. Using this method, we can also reduce the relay coil density.

Even in a high VWC environment, a robust communication can still be established.

As mentioned in the "System Design" section, a 3D MI coil is designed to cover the 3D space in the underground environment. The last step of our experiment is to use the testbed to measure the PER for 3D MI coils. A comparison of PER between 1D and 3D MI coils in different underground environments is shown in Figure 22. By deploying a 3D MI coil as the receiver with a distance of 2 m from transmitter and transmitting a series of packets, PER can be measured with intersection angle and VWC changing. We also measure the PER for the original MI coil to make a comparison. In this experiment, both original and 3D receiving coils are rotated to change the intersection angle to the transmitting coil. By rotating the receiving coils from 0 degree to 180°, we try to find the blind spot of the communication. In Figure 22(a), the original MI coils suffer from a high PER when two coils are deployed orthogonally to each other (90°), especially in the high VWC environment. However, by using the 3D MI coil, no matter how we change the intersection angle, the PER is kept at a low level throughout the experiments. Even in a high VWC environment, a robust communication can still be established.

CONCLUSION

In this article, we develop a testbed of different MI-based underground communication systems, which validates the feasibility and benefits of using MI for underground applications. First, the experimental measurements are compared with the calculated results based on the developed channel model. According to the experimental results, compared with using EM waves, a significant increase of signal

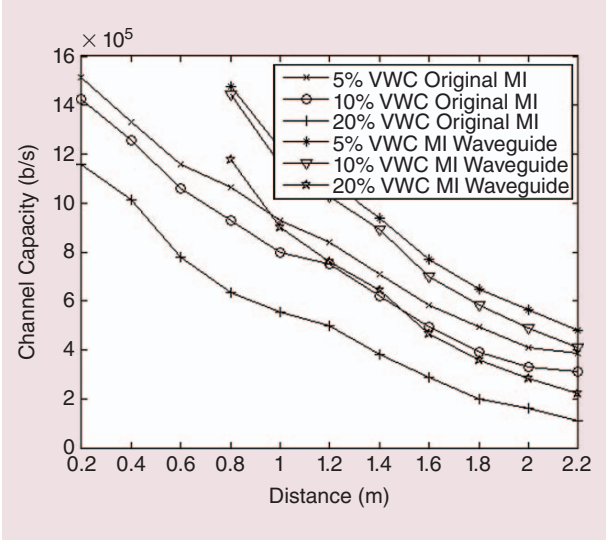

FIGURE 20. The channel capacity of MI communication in different underground environments.

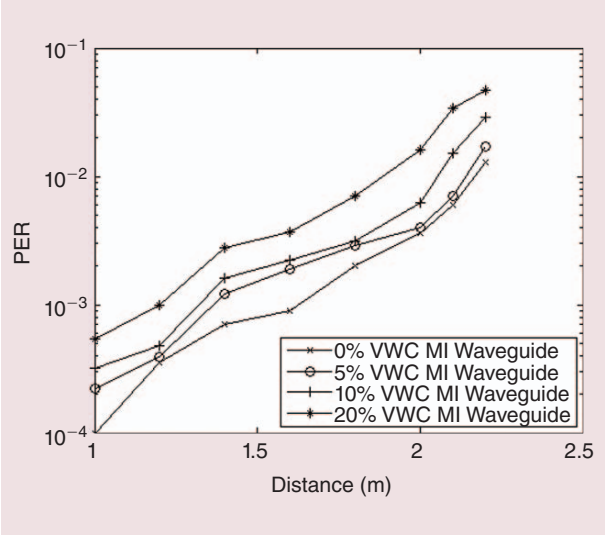

FIGURE 21. The PER of the MI waveguide in underground environments.

strength can be achieved using the MI technique, especially in cases with high VWC. By measuring the PER, we demonstrate that high-quality communication can be provided using the MI technique in underground environments. The testbed implements more advanced MI systems where the MI waveguide is used to extend the communication range and the 3D MI coil is used for omnidirectional coverage. For the MI waveguide, a significant improvement of received signal strength can be achieved and the bandwidth is not obviously influenced by the relays. A robust communication is established by using 3D MI coils that allow a low PER when rotating the receiver.

The GRC is a graphical user interface via which different blocks can be connected and then the codes generated in Python according to the connected blocks.

There is still room for improvements in future work: instead of handmade MI coil circuits, we plan to design PCBs to make the coils printed on boards so that the signal can be received more efficiently and accurately. The PCB-designed circuits will be applied in the fabrication of MI relays and 3D MI coils as well. To achieve the communication distance enlargement and 3D space coverage at the same time, we plan to design 3D MI relays to let the MI waveguide propagate omnidirectionally. To achieve this, a communication scheme should be developed first in this complicated case.

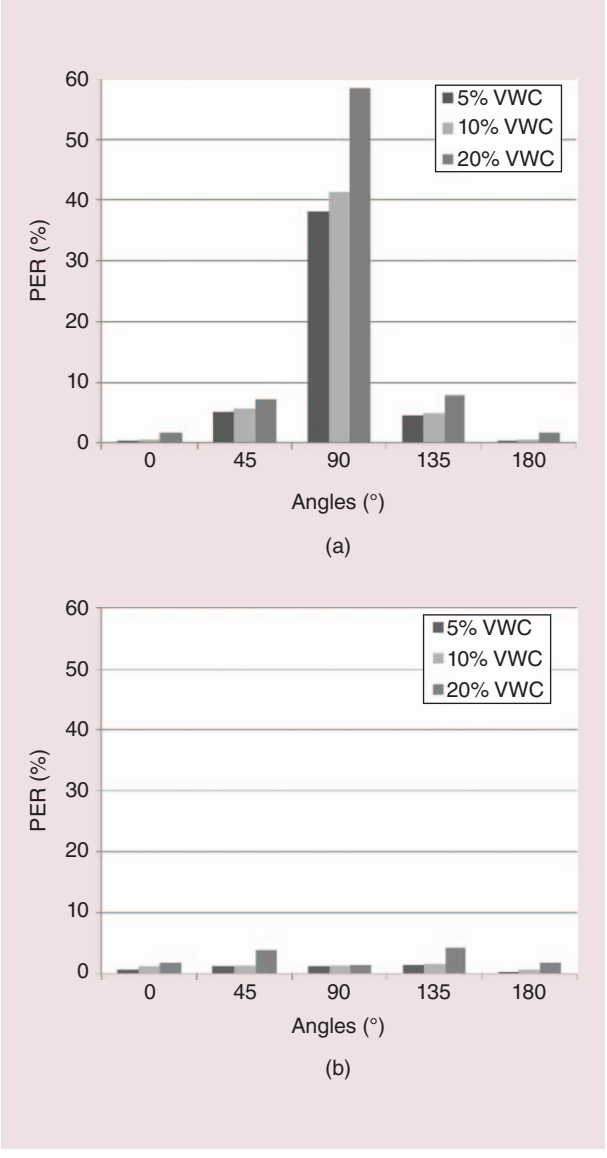

FIGURE 22. A comparison of PER between one-directional (1D) and 3D MI coils in different VWC underground environments: (a) 1D MI PER and (b) 3D MI PER.

ACKNOWLEDGMENT

This work is based on work supported by a start-up grant from the State University of New York at Buffalo and the U.S. National Science Foundation under grant 1320758.

AUTHOR INFORMATION

Xin Tan (xtan3@buffalo.edu) received his B.S. degree in automation from the Beijing Institute of Technology, China, and his M.S. degree in electrical engineering from the State University of New York at Buffalo in 2011 and 2013, respectively. Currently, he is a Ph.D. student in the Department of Electrical Engineering at the State University of New York at Buffalo. His current research interests are in wireless communications and wireless sensor networks. He is a Student Member of the IEEE.

Zhi Sun (zhisun@buffalo.edu) received his B.S. degree in telecommunication engineering from the Beijing University of Posts and Telecommunications, and his M.S. degree in electronic engineering from Tsinghua University, Beijing, China, in 2004 and 2007, respectively. He received his Ph.D. degree in electrical and computer engineering from the Georgia Institute of Technology, Atlanta, in 2011. Currently, he is an assistant professor in the Department of Electrical Engineering at the State University of New York at Buffalo. Prior to that, he was a postdoctoral fellow at the Georgia Institute of Technology. He was a recipient of the Best Paper Award at the 2010 IEEE Global Communications Conference. He received the BWN Researcher of the Year Award at the Georgia Institute of Technology in 2009. He was also given the outstanding graduate award at Tsinghua University in 2007. His expertise and research interests lie in wireless communications, wireless sensor networks, and cyberphysical systems in challenged environments. He is a Member of the IEEE.

Ian F. Akyildiz (ian@ece.gatech.edu) received his B.S., M.S., and Ph.D. degrees in computer engineering from

the University of Erlangen Nurnberg, Germany, in 1978, 1981, and 1984, respectively. Currently, he is the Ken Byers Chair Professor in telecommunications with the School of Electrical and Computer Engineering, the director of the Broadband Wireless Networking Laboratory, and the chair of the Telecommunication Group, all at the Georgia Institute of Technology, Atlanta. Since 2013, he has been a Finland Distinguished Professor Program professor (supported by the Academy of Science) with the Department of Electronics and Communications Engineering, Tampere University of Technology, Finland; he is also the founding director of the Nano Communications Center there. Since 2008, he has been an honorary professor with the School of Electrical Engineering at the Universitat Politècnica de Catalunya, Barcelona, Spain, and is the founding director of the NaNoNetworking Center in Catalunya. Since 2011, he has been a consulting chair professor at the Department of Information Technology, King Abdulaziz University, Jeddah, Saudi Arabia. Akyildiz is the editor-in-chief of *Computer Networks*, and the founding editor-in-chief of *Ad Hoc Networks, Physical Communication*, and *Nano Communication Networks*. He is a Fellow of the IEEE (1996) and an ACM fellow (1997). He received numerous awards from the IEEE and ACM. His current research interests are in software-defined networks, nanonetworks, terahertz band, fifth-generation cellular systems, and wireless sensor networks in challenged environments.

REFERENCES

[1] A. Markham and N. Trigoni, "Magneto-inductive networked rescue system (miners) taking sensor networks underground," in *Proc. 11th Int. Conf. Information Processing Sensor Networks*, 2012, pp. 317–328.

[2] A. R. Silva and M. C. Vuran, "Empirical evaluation of wireless underground-to-underground communication in wireless underground sensor networks," *Distrib. Comput. Sensor Syst.*, 2009, pp. 231–244.

[3] H. Guo and Z. Sun, "Channel and energy modeling for self-contained wireless sensor networks in oil reservoirs," *IEEE Trans. Wireless Commun.*, vol. 13, pp. 2258–2269, Mar. 2014.

[4] I. F. Akyildiz and E. P. Stuntebeck, "Wireless underground sensor networks: Research challenges," *Ad Hoc Netw.*, vol. 4, no. 6, pp. 669–686, Nov. 2006.

[5] M. Li and Y. Liu, "Underground structure monitoring with wireless sensor networks," in *Proc. 6th Int. Conf. Information Processing Sensor Networks*, 2007, pp. 69–78.

[6] X. Tan and Z. Sun, "An optimal leakage detection strategy for underground pipelines using magnetic induction-based sensor networks," in *Wireless Algorithms, System, and Application*, vol. 7992. Berlin, Germany: Springer, 2013, pp. 414–425.

[7] Z. Sun, P. Wang, M. C. Vuran, M. A. AI-Rodhaan, A. M. AI-Dhelaan, and I. F. Akyidiz, "MISE-PIPE: Magnetic induction-based wireless sensor networks for underground pipeline monitoring," *Ad Hoc Netw.*, vol. 9, no. 3, pp. 218–227, May 2011.

[8] Z. Sun and I. F. Akyildiz, "Magnetic induction communications for wireless underground sensor networks," *IEEE Trans. Antennas Propag.*, vol. 58, pp. 2426–2435, July 2010.

[9] I. F. Akyildiz, Z. Sun, and M. C. Vuran, "Signal propagation techniques for wireless underground communication networks," *Phys. Commun.*, vol. 2, no. 3, pp. 167–183, Sept. 2009.

[10] Z. Sun and I. F. Akyildiz, "On capacity of magnetic induction-based wireless underground sensor networks," in *Proc. IEEE INFOCOM*, Orlando, FL, Mar. 2012, pp. 370–378.

[11] Z. Sun, I. F. Akyildiz, S. Kisseleff, and W. Gerstacker, "Increasing the capacity of magnetic induction communications in RF-Challenged environments," *IEEE Trans. Commun.*, vol. 61, no. 9, pp. 3943–3952, Sept. 2013.

[12] Z. Tong, M. S. Arifianto, and C. F. Liau, "Wireless transmission using universal software radio peripheral," in *Proc. Int. Conf. Space Science Communication,* Oct. 2009, pp. 19–23.

[13] M. C. Vuran and I. F. Akyildiz, "Channel model and analysis for wireless underground sensor networks in soil medium," *Phys. Commun.*, vol. 3, no. 4, pp. 245–254, Dec. 2010.

[14] X. Dong and M. C. Vuran, "A channel model for wireless underground sensor networks using lateral waves," in *Proc. IEEE GLOBECOM*, Dec. 2011, pp. 1–6.

[15] A. R. Silva and M. C. Vuran, "Development of a testbed for wireless underground sensor networks," *J. Wireless Commun. Netw.*, vol. 2010, no. 9, article 620307, 2010.

[16] Z. Sun and I. F. Akyildiz, "Deployment algorithms for wireless underground sensor networks using magnetic induction," in *Proc. IEEE GLOBECOM*, Dec. 6–10, 2010, pp. 1–5.

[17] C. J. Stevens, C. W. T. Chan, K. Stamatis, and D. J. Ewards, "Magnetic Metamaterials as 1-D data transfer channels: An application for magneto-inductive waves," *IEEE Trans. Microwave Theory Tech.*, vol. 58, no. 5, pp. 1248–1256, 2010.

[18] F. Zhang, S. A. Hackworth, W. Fu, C. Li, Z. Mao, and M. Sun, "Relay effect of wireless power transfer using strong coupled magnetic resonances," *IEEE Trans. Magn.*, vol. 47, no. 5, pp. 1478–1481, May 2011.

[19] M. C. K. Wiltshire, E. Shamonina, I. R. Young, and L. Solymar, "Dispersion characteristics of magneto-inductive waves: Comparison between theory and experiment," *Electron. Lett.*, vol. 39, no. 2, pp. 215–217, 2003.

[20] R. R. A. Syms, E. Shamonina, and L. Solymar, "Magneto-inductive waveguide devices," *IEE Microwaves Antennas Propag.*, vol. 153, no. 2, pp. 111–121, 2006.

[21] R. R. A. Syms, I. R. Young, and L. Solymar, "Low-loss magneto-inductive waveguides," *J. Phys. D: Appl. Phys.*, vol. 39, pp. 3945–3951, 2006.

[22] S. Cheon, Y.-H. Kim, S.-Y. Kang, M. L. Lee, and T. Zyung, "Wireless energy transfer system with multiple coils via coupled magnetic resonances," *ETRI J.*, vol. 34, no. 4, pp. 527–535, Aug. 2012.

[23] B. Wang, W. Yerazunis, and K. H. Teo, "Wireless power transfer: Metamaterials and array of coupled resonators," *Proc. IEEE*, vol. 101, no. 6, pp. 0018–9219, June 2013.

[24] A. Karalis, J. D. Joannopoulos, and M. Soljacic, "Efficient wireless non-radiative mid-range energy transfer," *Annals Phys.*, vol. 323, no. 1, pp. 34–48, 2008.

[25] C. K. Lee, W. X. Zhang, and S. Y. R. Hui, "Effects of magnetic coupling of nonadjacent resonators on wireless power domino-resonator systems," *IEEE Trans. Power Electron.*, vol. 27, no. 4, pp. 1905–1916, Apr. 2012.

[26] R. Carta, M. Sfakiotakis, N. Pateromichelakis, J. Thone, D. P. Tsakiris, and R. Puers, "A multi-coil inductive powering system for an endoscopic capsule with vibratory actuation," *Sens. Actuators A, Phys.*, vol. 172, no. 1, pp. 253–258, 2011.

[27] W. Zhong, C. K. Lee, and S. Y. R. Hui, "General analysis on the use of tesla's resonators in domino forms for wireless power transfer," *IEEE Trans. Ind. Electron.*, vol. 60, no. 1, pp. 261–270, Jan. 2013.

[28] X. Zhang, S. L. Ho, and W. N. Fu, "Quantitative design and analysis of relay resonators in wireless power transfer system," *IEEE Trans. Magn.*, vol. 48, no. 11, pp. 4026–4029, Nov. 2012.